J. Fluid Mech. (1992), *vol.* 244, *pp.* 377–404

Unsteady transonic flow past a quarter-plane

By N. PEAKE

Department of Applied Mathematics and Theoretical Physics, University of Cambridge, Silver Street, Cambridge CB3 9EW, UK

(Received 19 February 1992 and in revised form 23 June 1992)

One of the most significant mechanisms of noise generation in prototype counter-rotation propeller systems is the unsteady interaction between the rear row and the wake and trailing tip vortices shed by the front row. A crucial part of predicting this noise is the determination of the resulting unsteady lift distribution on the rear row; since much of the interaction occurs in the vicinity of the rear-row blade tips, however, two-dimensional airfoil response theory cannot be applied exclusively, and some account of the presence of the blade tip must be taken. With this in mind, we solve the model problem of the unsteady interaction between a convected harmonic velocity gust and a quarter-plane, for the case of mean flow Mach number in the transonic range. The detailed lift distribution near the leading edge and corner is analysed, revealing the complicated nature of the lift singularity at the corner, and allowing the lift distribution throughout a narrow region along the leading edge to be determined. A closed-form expression for the practically important acoustically weighted lift is derived, which could easily be incorporated into existing noise prediction schemes in order to correct the rear-row blade response calculations for the presence of the blade tips. The radiation in this quarter-plane problem is also considered, and the field is seen to possess two components, one arising from the interaction between the gust and the semi-infinite leading edge, and the other from the interaction between the gust and the blade corner. The acoustic energy associated with this second term, corresponding to the conversion of vortical energy into sound by the corner, is considered in detail, and the directivity and parametric scaling determined. Our exact solution to this model problem is also used to assess the accuracy of a strip-theory approximation, which is seen to be accurate in this case over only a restricted range of observer positions.

1. Introduction

The development of two-stage, counter-rotation propeller systems (or *propfans*) as possible powerplants for future passenger aircraft has raised a number of technical difficulties, not least of which being the often unacceptably high noise levels produced by such systems. One of the most potent mechanisms of sound generation is the interaction between the two, closely spaced, blade rows; the wake and vortex structures shed by the front row impinge on the rear row, leading to an unsteady lift distribution on the rear row, and thereby producing radiation (termed *interaction noise*).

The disturbance field produced by the motion of the forward blade row contains a number of components; the potential field of the front-row blades is small, however (since propfan blades are typically thin), and it is the wake and tip vortices shed by the front-row blades which dominate the interaction with the rear row. Prediction of the interaction noise therefore falls into two stages; first, the wake and vorticity

distribution shed by the front-row blades must be calculated; and second, the response of the rear blade row to its interaction with these disturbances must be analysed. The structure of the propfan wake has been investigated experimentally by Reynolds (1979), by Sundar & Sullivan (1986) and by Hanson & Patrick (1989), whilst experiments on the tip vortex have been reported by Vaczy & McCormick (1987) and by Simonich, McCormick & Lavrich (1989); as yet little is known quantitatively about either the wake or the tip vortex, although some information can be inferred by comparison with the better-understood case of wing theory. The structure of the wake and tip vortex will not be the concern of this paper, however, and we shall consider only the response of the rear row to some known wake or vorticity distribution, which we shall suppose has been predetermined, either by computation or experimentally.

Since the wake and the vorticity distribution are periodic in space and time (given the assumed regularity of the front-row blading), we need consider only the scattering of a single Fourier component by the rear row; the radiation produced by the interaction with the full wake and tip vortices can then be recovered by summing the contributions from each of these harmonic components. As a first approximation we will neglect the propeller rotation and work in a blade-fixed frame, in which case this single Fourier component corresponds to a harmonic velocity gust convected by uniform mean flow. It is clear that, whilst analysis of this rectilinear motion will be inappropriate for determining the (far-field) radiation produced by a rotating blade, it will yield a good approximation for quantities which are evaluated close to the blade surface (in particular for the lift distribution), which are relatively insensitive to the fully three-dimensional rotational nature of the propeller flow. Once the lift distribution has been calculated in this way, the radiation produced by a rotating blade can be estimated using standard radiation integrals for rotating sources (see Parry & Crighton 1989*a*). We note here that modern propeller blades possess rounded and often highly swept tips, but in this paper we shall only consider (in common with the authors listed below) an unswept rectangular blade with sharp corners, as a first step in the analysis.

The problem of calculating the rear-row blade response has therefore been reduced to the consideration of the interaction between a harmonic velocity gust and an airfoil. The model problem of the scattering of a gust by a blade of finite chord, but infinite span, is considered by Amiet (1976) and by Martinez & Widnall (1980) (simplified formulae, assuming an infinite blade chord and no spanwise dependence in the incident gust, are given by Goldstein 1976). With particular relevance to the question of rear-row response to the tip vortex, Amiet (1986) considers the interaction between a line vortex and an infinite-span airfoil in subsonic mean flow, by adding together the appropriate combination of Fourier coefficients from his harmonic gust analysis, whilst Ffowcs Williams & Guo (1988) and Guo (1990) analyse the interruption of a constant-velocity core by an infinite-span blade in supersonic flow.

The above results cannot be applied directly to the problem of determining the rear-row unsteady lift distribution close to the blade tips, however, since here the effect of the blade corners will become significant, and the blade can no longer be assumed to possess an infinite span. The effects of the corners are important in calculating the response to the front-row wake, since whilst Parry & Crighton (1989*a*) have proved that the wake response is dominated by a critical radial station which lies inboard of the tip, it is often the case that for practical parameter values this point closely approaches the blade tip. However, inclusion of the blade corner is

crucial for the prediction of tip-vortex interaction noise, since the downwash on the rear blade row due to the presence of the tip vortex will be concentrated near the tips of the rear blades, given that the blade lengths in propfan systems are typically the same in front and rear rows. Solution of model problems concerning the unsteady interaction of a gust with a blade corner are therefore required, and some work has already been done. The related flutter problem of an oscillating quarter-plane (i.e. a plane which is semi-infinite in two perpendicular directions) can be solved exactly for supersonic mean flow (see Stewartson 1950 and Miles 1951). No exact solutions for subsonic flow have been found, however (due to the complicated nature of the upstream interaction of the corner), although an approximate solution is given by Martinez & Widnall (1983) (obtained by relaxing one of the boundary conditions), and a numerical scheme for determining the unsteady lift distribution on a semi-infinite blade is described by Chu & Widnall (1974). None of these results can be readily applied for the practically important case of mean flow in the transonic range (the blade tips of a propfan operating under cruise conditions will typically be moving transonically), however, since they essentially use a form of the small perturbation equation which is inappropriate for mean-flow Mach numbers close to unity (the transonic limit of the solution of the supersonic form of the small disturbance equation does not agree with the genuine linearized transonic solution; see Landahl 1989, p. 26).

In this paper we shall therefore derive a linearized solution for the interaction between a harmonic velocity gust and a quarter-plane in transonic mean flow, and consider the case of the gust reduced frequency, Ω, being large (we will take typically $\Omega \geqslant 5$); this corresponds to the situation commonly encountered with propfans. Throughout this paper we use the definition of reduced frequency

$$\Omega \equiv \omega c/U,$$

where ω is the gust frequency, c is the blade chord and U is the mean flow velocity. We apply a method described by Landahl (1989), which allows us to formulate a *transonic similarity law*, whereby the solution to the problem for mean flow Mach number, M, equal to unity can be related to the solutions for M close to unity. Landahl (1989) demonstrates that this procedure is valid for $|1-M| \ll \Omega$; for a given (large) reduced frequency our theory will therefore be valid over a non-trivial range of M, for M both greater than and less than unity. In this high-reduced-frequency case the effects of the blade trailing edge and hub region will be relatively unimportant and can be legitimately neglected in our analysis, justifying our representation of the finite chord blade by a quarter-plane. The problem considered in this paper represents an extension of the work of Cargill (1987), who dealt with the case of $M = 1$. We note here that whilst the investigation described in this paper has primarily been carried out with a view to understanding propfan noise, our model problem has application in other areas (for instance to the question of blade–vortex interaction on a helicopter, or the gust loading on an aircraft wing), and various parts of the analysis presented below have been performed with these situations in mind.

In §2 the mathematical formulation and derivation of the transonic similarity law are described, whilst in §3 the solution of the $M = 1$ problem is found using the Wiener–Hopf technique. Since the main aim of this paper is to determine the magnitude of the effects of the presence of the blade corner on the interaction, the solution of the corresponding problem for an infinite-span blade is presented in Appendix A for comparison. The lift distribution on the quarter-plane is analysed in §4; whilst it will not prove possible to determine an exact closed-form expression for

the detailed surface pressure distribution, asymptotic analysis can be applied for the two cases of points on the blade close to the corner, and points close to the leading edge but away from the corner. First, the nature of the singularity in the lift at the corner is revealed, the strength of which is seen to depend on the path along which the corner is approached. Second, the first two terms in the expansion of the lift distribution close to the leading edge are calculated; the leading term (representing the typical inverse-square-root singularity at a leading edge) is precisely that found for an infinite-span blade, and it is only in the second term (which is finite at the leading edge) that the effects of the corner become apparent. The combination of these two sets of asymptotic formulae allows us to specify the detailed lift distribution throughout a strip of width $O(\Omega^{-1})$ along the leading edge (including the corner region), and this might well be of some practical interest, since this is precisely the part of the blade which is most important in sound generation by either propellers or helicopters. The results in this section might also provide a benchmark test of the accuracy of the various CFD-based codes currently being envisaged for rotor noise prediction.

In §5 an explicit closed-form expression for the *acoustically weighted lift* per unit span, which corresponds to the effective lift on the blade for the purpose of noise generation, is derived, and the effect of the presence of the corner is seen to appear explicitly in this quantity in the form of an error-function factor. Considerable simplification of propeller noise prediction is possible by use of the fact that the blade number, B, is large is modern systems (typically 7 or 8), allowing application of asymptotic analysis in the limit $B \to \infty$; see Parry & Crighton (1989*b*), Peake & Crighton (1991) for details of the use of the large-B approximation in determining the noise of a single-rotation propeller, and Parry & Crighton (1989*a*) for its use in predicting the noise of a counter-rotation propeller. This limit can also be applied in our analysis, in which case the acoustically weighted lift on a real, finite-chord blade reduces to that on our quarter-plane (determined in §5), and full details are given in Appendix B. The practical importance of the result of §5 is that it provides an algebraic correction factor, whereby the effects of the presence of the blade corner can be incorporated easily and efficiently into existing propfan noise prediction codes which rely on two-dimensional response theory (e.g. Parry & Crighton's 1989*a* scheme for predicting wake interaction noise).

In §6 the far-field form of the pressure is calculated for our quarter-plane problem; whilst, as has already been noted, such results cannot be applied to the question of propeller noise, they are relevant to the issue of noise generation by the interaction between an aircraft wing in rectilinear motion and a gust. The noise is seen to possess two components; one (two-dimensional) contribution arises from the interaction of the gust with the semi-infinite leading edge, and corresponds exactly to the field that would be produced by an infinite-span blade; whilst the second (fully three-dimensional) component is generated purely by the interaction with the blade corner. It is this second term which is of the greater interest, since we are concerned here with the effects of the presence of the blade corner on the scattering of the gust. The conversion of vortical to acoustic energy by the corner interaction can therefore be assessed by considering the energy intensity associated with this second term, and expressions for the directivity and parametric scaling are derived.

In §7 the accuracy of a strip-theory approximation in predicting the radiation in our model problem is assessed, and it is seen that the strip theory will only yield an accurate result for a restricted range of observer positions. However, our analysis does yield a simple algebraic factor, whereby the strip-theory results can be corrected

for the presence of the corner; this might be of some practical significance, since more complicated gust–wing problems (possibly involving mean loading or thickness effects) could be completed using strip theory, and the results then corrected for the presence of the wing tip using this factor.

Finally, it is worth remarking that the material described in this paper builds on the foundations laid by Cargill (1987). The new work presented here includes the generalization of Cargill's analysis to $M \neq 1$ (§2), the detailed elucidation of the structure of the corner singularity and the lift distribution near the leading edge (§4), the prediction of the spanwise lift distribution (§5) and the consideration of the acoustic intensity of the scattered field (§6). The Fourier transform and basic solution of the equations is given explicitly by Cargill (1987), but presented here in §3 for completeness, whilst the derivation of expressions for the acoustic pressure (§6) and the strip-theory approximation (§7) represent extensions of ideas already outlined by Cargill.

2. Mathematical formulation

We consider a rigid semi-infinite blade, which is symmetric about the plane $z = 0$, has its semi-infinite leading edge aligned along the positive (spanwise) y-axis and its side edge aligned along the (chordwise) x-axis; the blade leading corner is at the origin; see figure 1. The blade chord length is c, independent of y, and we will suppose that the blade is thin, with the thickness-to-chord ratio $\epsilon \ll 1$. The role of c will be in the definition of the reduced frequency of the system, and in normalizing the coordinates; once this has been done we shall subsequently neglect the effects of the blade trailing edge, thereby taking the chord to be effectively infinite. There is a uniform mean flow relative to the blade of speed U parallel to the x-axis, where U will be close to the quiescent sound speed c_0 of the surrounding medium. A harmonic velocity gust, corresponding to a small perturbation to the velocity in the z-direction, and representing a component of some incident vorticity distribution, is convected from upstream by the mean flow and has frequency ω (we consider the case of ω large, so that the wavelength of the gust is much less than the blade chord). We non-dimensionalize the problem by dividing all lengths by the chord c, velocities by U and time by c/U, and the velocity downwash on the blade due to the gust then becomes

$$V \exp(\mathrm{i}\Omega t - \mathrm{i}\Omega x - \mathrm{i}k_y y)\, \boldsymbol{z},$$

where V is the normalized magnitude of the gust, $\boldsymbol{z}$ is a unit vector in the z-direction, Ω is the reduced frequency (i.e. $\Omega = c\omega/U$) and k_y is the wavenumber of the gust in the y-direction (we note that the x wavenumber is precisely Ω, since the convected gust must have a zero associated pressure). We suppose further that $V \ll 1$, so that the perturbation, $\boldsymbol{u}$, to the mean flow resulting from the interaction between the gust and the blade is irrotational, with $\boldsymbol{u} = \nabla\varphi$, and where $\varphi(x, y, z, t)$ satisfies the small-disturbance equation (see Landahl 1989 for full details)

$$[1 - M^2 - M^2(\gamma+1)\varphi_x]\varphi_{xx} + \varphi_{yy} + \varphi_{zz} - 2M^2\varphi_{xt} - M^2\varphi_{tt} = 0; \tag{1}$$

M is the mean flow Mach number and γ is simply the ratio of specific heats of an ideal gas (having assumed that the flow is isentropic). The next step (as described by Landahl 1989) is to write $\varphi(x, y, z)$ as the sum of a steady part $\phi_1(x, y, z)$, which is symmetric about the $z = 0$ plane and corresponds to the distortion of the mean flow by the blade thickness, and an unsteady part $\phi_2(x, y, z)\exp(\mathrm{i}\Omega t)$ generated by the unsteady interaction of the blade with the harmonic velocity gust. We consider

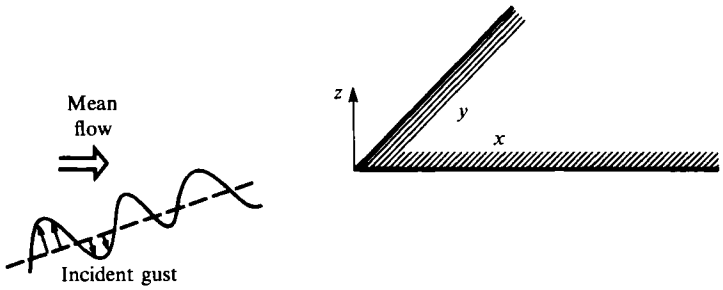

FIGURE 1. The coordinate system.

the situation in which $V \ll \epsilon$ (i.e. the magnitude of the incident gust is much less than the blade thickness) so that the unsteady part of the flow, ϕ_2, can be treated as a small perturbation to the steady disturbance, ϕ_1, allowing the partial linearization of (1) in the form

$$\{[(1-M^2)-M^2(\gamma+1)\phi_{1x}]\phi_{2x}-2i\Omega M^2\phi_2\}_x+\phi_{2yy}+\phi_{2zz}+M^2\Omega^2\phi_2=0. \tag{2}$$

In a naive linearization of (2) one would simply neglect the term containing ϕ_{1x}, yielding the usual convected wave equation of linear acoustics, namely

$$(1-M^2)\phi_{2xx}+\phi_{2yy}+\phi_{2zz}-2i\Omega M^2\phi_{2x}+M^2\Omega^2\phi_2=0, \tag{3}$$

which is the equation considered by Miles (1951) and Stewartson (1950). In the transonic regime considered in this paper it is not appropriate to apply (3), however, since the transonic solution is not recovered uniformly by applying the limit $M\to 1$ in (3) (Landahl 1989, pp. 26–30 demonstrates that in two dimensions the limiting value of the solution of (3) as $M\to 1+$ does not agree with the transonic solution, whilst the transonic solution is regained in the limit $M\to 1-$). The appropriate unsteady transonic linearization of (2) is described by Landahl and in more detail by Miles (1954). For a three-dimensional planar body we have that $\phi_{1x}=O(\epsilon)$, and following Miles (1954) we impose the restriction that $\epsilon \ll \Omega^{\frac{3}{2}}$ (which is clearly satisfied for our thin blade in a moderate-frequency gust); the terms in curly brackets in (2) will now be dominated by the unsteady linear term provided that $\Omega \gg |1-M|$, yielding the final fully linearized unsteady disturbance equation

$$\phi_{2yy}+\phi_{2zz}-2i\Omega M^2\phi_{2x}+\Omega^2M^2\phi_2=0. \tag{4}$$

Equation (4) can therefore be applied for combinations of Ω and M for which $\Omega \gg |1-M|$, and since propeller noise is typically of high frequency anyway (due to the relatively large number of blades in modern systems – see (B 1)), this will not be a significant restriction, and our theory will be applicable to a non-trivial range of Mach numbers about $M=1$. It should also be noted that the standard thin-blade approximation of applying the normal velocity boundary condition on the mean plane $z=0$, rather than on the genuine blade surface, can also be applied for our thin blade, and full details are again given in Landahl (1989). It has been implicit in our derivation that the solution of (4) is in fact only the first term in a series expansion of $\phi_2(x,y,z)$; the term in square brackets in (2) will generate higher-order terms, the largest of which is a factor $O(1-M)$ smaller than this first term. In our transonic regime we can therefore neglect these higher-order terms as small, and consider only the solution of (4), which provides the dominant contribution to the unsteady transonic flow.

In this paper our primary concern is with the effect of the blade leading edge and corner, and in what follows we shall neglect the effects of the trailing edge, thereby replacing the finite-chord blade by an infinite quarter-plane lying in the first quadrant of the (x, y)-plane; for the large-Ω values we consider, for which the blade chord is much longer than the wavelength of the incident gust and trailing-edge effects are small, this will be a good approximation. The system is shown in figure 1. Thus, in order to calculate the unsteady disturbance $\phi_2(x, y, z)$ we must solve (4) subject to

(i) the total normal velocity on the quarter-plane is zero, i.e.

$$\phi_{2z}(x, y, 0) + V \exp(-\mathrm{i}\Omega x - \mathrm{i}k_y y - \epsilon y) = 0 \quad \text{for} \quad x > 0, y > 0,$$

where $\epsilon > 0$ is a small fictitious dissipation which will be set to zero at the end of the calculation;

(ii) because the unsteady potential is antisymmetric in z, and a jump in the unsteady pressure can only be supported across the rigid quarter-plane, we have $\phi_2(x, y, 0) = 0$ away from the quadrant $x > 0, y > 0$;

(iii) the solution must satisfy a radiation condition, i.e. be composed of outgoing waves at infinity.

Since we shall no longer be concerned with the steady part of the flow, we drop the suffix 2 in what follows, and refer to the unsteady potential simply as $\phi(x, y, z)$. The solution of (4) subject to the above boundary conditions, for general values of M in the transonic regime, can be related to the $M = 1$ solution via a transonic similarity law (again see Landahl 1989); the substitution $y = \tilde{y}/M$, $z = \tilde{z}/M$ reduces (4) to its $M = 1$ form, so that by replacing k_y by $k_y M$ and dividing $\phi(x, y, z)$ by M in boundary condition (i) we cast the problem into precisely its $M = 1$ form (boundary conditions (ii) and (iii) are unaffected by this process). Writing the unsteady potential in a form which makes clear its parametric dependence on the flow, we see that

$$\phi(x, y, z, \Omega, k_y, M) = M^{-1}\phi(x, My, Mz, \Omega, k_y/M, 1), \tag{5}$$

which demonstrates that the potential for general transonic M is simply related to the potential for $M = 1$, once the correct modifications of the y- and z-coordinates and the transverse gust wavenumber have been made. We are therefore left to solve the problem for $M = 1$, and then apply our transonic similarity law to find the solution for the more general case $M \neq 1$.

3. Solution of the $M = 1$ problem

In this section we shall solve (4) subject to the boundary conditions (i), (ii) and (iii) for $M = 1$, and our method of solution will be the Wiener–Hopf technique; this has previously been presented by Cargill (1987). Strictly speaking, the Wiener–Hopf analysis must be completed by first supposing that the reduced frequency possesses a small negative imaginary part, Ω_1, which is set to zero at the end of the analysis (this allows a narrow strip to be defined along the real axis, in which the various Fourier transforms are analytic). However, for clarity we shall suppose $\Omega_1 = 0$ from the outset; in the present problem this will have no effect on the results. We define the double Fourier transform

$$\Phi(k_1, k_2, z) = \int_{-\infty}^{\infty} \int_{-\infty}^{\infty} \phi(x, y, z) \exp(\mathrm{i}k_1 x + \mathrm{i}k_2 y)\, \mathrm{d}x\, \mathrm{d}y, \tag{6}$$

so that transforming (4) yields

$$\Phi_{zz} - \gamma^2 \Phi = 0, \tag{7}$$

where $$\gamma^2(k_1, k_2) \equiv k_2^2 + 2\Omega k_1 - \Omega^2. \tag{8}$$

We will be performing our Wiener–Hopf analysis with respect to the k_2 transform variable, and a key step will be the multiplicative factorization of $\gamma(k_1, k_2)$; at this point we therefore write $\gamma(k_1, k_2)$ in the form $\gamma(k_1, k_2) = \gamma^+(k_1, k_2)\,\gamma^-(k_1, k_2)$, with $\gamma^\pm(k_1, k_2)$ analytic and non-zero in the upper and lower halves of the complex k_2-plane respectively, and find that

$$\gamma^\pm(k_1, k_2) = (k_2 \pm \mathrm{i}(2\Omega k_1 - \Omega^2)^{\frac{1}{2}})^{\frac{1}{2}}. \tag{9}$$

The branch cut in the k_1-plane is chosen to lie between $\frac{1}{2}\Omega$ and infinity in the lower half-plane, parallel to the negative imaginary axis (with the square root real and positive as $k_1 \to +\infty$ along the real axis); whilst in the k_2-plane cuts are chosen originating from $\pm\mathrm{i}(2\Omega k_1 - \Omega^2)^{\frac{1}{2}}$ and joining to infinity through the upper and lower half-planes respectively (this ensures that the $\gamma^\pm(k_1, k_2)$ defined in (9) are analytic in the correct half-planes); $\gamma(k_1, k_2)$ is again chosen to be real and positive as $k_2 \to +\infty$ along the real axis. Transforming the normal velocity boundary condition (i) leads to

$$\Phi_z^+(k_1, k_2, 0) - \frac{V}{(k_1 - \Omega)(k_2 - k_y + \mathrm{i}\epsilon)} = 0, \tag{10}$$

where the $+$ superfix on $\Phi_z^+(k_1, k_2, 0)$ indicates that the k_2 integral has been completed over the positive semi-infinite range (i.e. $0 \leqslant k_2 < \infty$); $\Phi_z^+(k_1, k_2, 0)$ is analytic in the upper-half of the k_2-plane. In deriving (10) we have used the fact that, for this $M = 1$ case, the quarter-plane exerts no upstream influence, so that $\phi_z(x, y, z)$ vanishes for $x < 0$. Since $\phi(x, y, z)$ is an odd function of z, (7) can easily be solved to give

$$\Phi(k_1, k_2, z) = \tfrac{1}{2}\,\mathrm{sgn}\,(z)\,[\Phi(k_1, k_2, 0)]_-^+ \exp(-\gamma|z|), \tag{11}$$

where $[\Phi(k_1, k_2, 0)]_-^+$ is simply the jump in $\Phi(k_1, k_2, 0)$ across $z = 0$, and it follows from boundary condition (ii) that $[\Phi(k_1, k_2, 0)]_-^+$ is analytic in the upper-half of the complex k_2-plane. Substituting (11) into (10) yields the Wiener–Hopf equation

$$\begin{aligned}
&\tfrac{1}{2}\gamma^+(k_1, k_2)\,[\Phi(k_1, k_2, 0)]_-^+ + \frac{V}{(k_1 - \Omega)(k_2 - k_y + \mathrm{i}\epsilon)\,\gamma^-(k_1, k_y - \mathrm{i}\epsilon)} \\
&\quad = -\frac{1}{\gamma^-(k_1, k_2)}\,\Phi_z^-(k_1, k_2, 0) - \frac{V}{(k_1 - \Omega)(k_2 - k_y + \mathrm{i}\epsilon)}\left[\frac{1}{\gamma^-(k_1, k_2)} - \frac{1}{\gamma^-(k_1, k_y - \mathrm{i}\epsilon)}\right] \\
&\quad \equiv E(k_2).
\end{aligned} \tag{12}$$

Following the standard Wiener–Hopf procedure (see Noble 1958, pp. 52–58), we now note that the left-hand side of (12) is analytic in the upper-half of the complex k_2-plane, whilst the right-hand side is analytic in the lower half-plane, and that by analytic continuation (12) therefore defines a function, $E(k_2)$, which is analytic in the whole k_2-plane. By choosing the least singular solution for $\phi(x, y, z)$, it follows that $E(k_2) \equiv 0$, yielding an expression for $[\Phi(k_1, k_2, 0)]_-^+$. The pressure associated with $\phi(x, y, z)$, denoted $p(x, y, z)$, is found from the usual relation of potential theory (i.e. $p(x, y, z) = -\mathrm{i}\Omega\phi - \phi_x$), and it follows that $[P(k_1, k_2, 0)]_-^+$, the Fourier transform of the pressure jump across $z = 0$, is given by

$$[P(k_1, k_2, 0)]_-^+ = -\frac{2\mathrm{i}V}{(k_2 - k_y + \mathrm{i}\epsilon)\,\gamma^+(k_1, k_2)\,\gamma^-(k_1, k_y - \mathrm{i}\epsilon)}. \tag{13}$$

From the antisymmetry of $\phi(x, y, z)$ about the plane $z = 0$, we note that the Fourier transform of the surface pressure, denoted $P(k_1, k_2, 0)$, is precisely $\frac{1}{2}[P(k_1, k_2, 0)]^{\pm}_{-}$. The detailed lift distribution on the blade is now found by inverting (13), to give

$$[p(x, y, 0)]^{+}_{-} = -\frac{\mathrm{i}V}{2\pi^2}\int_{k_1}\int_{k_2}\frac{\exp(-\mathrm{i}k_1 x - \mathrm{i}k_2 y)}{(k_2 - k_y)\,\gamma^{+}(k_1, k_2)\,\gamma^{-}(k_1, k_y)}\,\mathrm{d}k_2\,\mathrm{d}k_1. \tag{14}$$

In (14), the integration contour in the k_2-plane lies below any singularity in the left-hand half-plane, and above any in the right-hand half-plane (given our choice of branch cuts this means that for $k_1 > \frac{1}{2}\Omega$ the k_2 contour is the real axis, whilst for $k_1 < \frac{1}{2}\Omega$ it is the real axis indented below the branch point at $k_2 = -|2\Omega k_1 - \Omega^2|$ and above the branch point at $k_2 = |2\Omega k_1 - \Omega^2|$); the integration contour in the k_1-plane is the real axis, indented above any branch points. It is easy to check that this choice of contours, together with the branch cuts chosen following (9), yields a solution which satisfies the radiation condition, and which vanishes in $x < 0$. In deriving (14) from (13) the role of the fictitious dissipation, ϵ, has been in determining the path of the integration contour relative to the various singularities; once this had been completed we set $\epsilon = 0$.

An integral expression for the potential can also be found in the form

$$\phi(x, y, z) = -\frac{\mathrm{sgn}(z)\,V}{4\pi^2}\int_{k_1}\int_{k_2}\frac{\exp(-\mathrm{i}k_1 x - \mathrm{i}k_2 y - \gamma|z|)}{(k_2 - k_y)\,\gamma^{+}(k_1, k_2)\,\gamma^{-}(k_1, k_y)\,(k_1 - \Omega)}\,\mathrm{d}k_2\,\mathrm{d}k_1, \tag{15}$$

where the k_2 contour is as before, and the k_1 contour is now indented above the pole at $k_1 = \Omega$. We emphasize that (14) and (15) have been derived for the case $M = 1$, and application of the transonic similarity law will be postponed until later sections.

4. The unsteady lift on the blade

In this section we consider the detailed lift distribution on the quarter-plane caused by its unsteady interaction with the gust, and will be concerned only with the portion of the blade close to the leading edge; this is the region which is most important in sound generation due to the presence of the leading-edge singularity in the lift, together with the effects of phase cancellation away from the edge in our high-frequency regime. The first step is to simplify (14) by making the substitution $k_1 = k_1' + \frac{1}{2}\Omega$. For $y < 0$ we close the k_2 integration contour in the upper half-plane, yielding zero lift (since the integrand is analytic in the upper half of the k_2-plane), as expected. Alternatively, for $y > 0$ we deform the k_2 integration contour round the branch cut in the lower half-plane (that is, the branch cut originating from $k_2 = -\mathrm{i}(2\Omega k_1')^{\frac{1}{2}}$), yielding both a branch-line integral and a residue contribution from the pole at $k_2 = k_y$. The branch line integral can be completed using a standard result (Gradshteyn & Ryzhik 1980, p. 338, 3.466(1)), and adding the pole and branch-line contributions together we find that

$$[p(x, y, 0)]^{+}_{-} = -\frac{V}{\pi}\exp(-\tfrac{1}{2}\mathrm{i}\Omega x)\int_{k_1'}\exp(-\mathrm{i}k_1' x - \mathrm{i}k_y y)\frac{\mathrm{erf}(\exp(-\frac{1}{4}\mathrm{i}\pi)\,y^{\frac{1}{2}}\gamma^{+}(k_1', k_y))}{\gamma(k_1', k_y)}\,\mathrm{d}k_1', \tag{16}$$

where the error function $\mathrm{erf}(z)$ is defined by (Abramowitz & Stegun 1968)

$$\mathrm{erf}(z) \equiv \frac{2}{\pi^{\frac{1}{2}}}\int_0^z \exp(-z'^2)\,\mathrm{d}z'.$$

Equation (16) is still valid only for $M = 1$, and has previously been derived by Cargill (1987).

For $x < 0$ we close the integration contour in (16) in the upper-half of the k_1'-plane, and since the integrand is analytic here (both k_1' branch cuts were chosen to lie below the real axis) we see that $[p(x,y,0)]^+_- = 0$ for $x < 0$, again as expected. In what follows we therefore consider only $x > 0$. It will not prove possible to derive a closed-form expression for the lift distribution $[p(x,y,0)]^+_-$ from the complicated integral in (16), but asymptotic analysis can be completed for either x and y small or for x small and y held fixed, and will fall into two stages. In §4.1 below we consider for simplicity the case of $k_y = 0$, and study the behaviour of the lift near the corner of the quarter-plane; whilst in §4.2 we find the first two terms in the expansion of $[p(x,y,0)]^+_-$, in the limit $x \to 0$ with y non-zero and held fixed (that is, the behaviour of the lift near the leading edge but not too close to the corner), this time with $k_y \neq 0$. By combining the results of §§4.1 and 4.2 we are able to specify the lift distribution throughout a strip of width $O(\Omega)^{-1}$ along the blade leading edge; it is again emphasized that this should be of practical interest, since the leading edge is the most significant region of the blade in terms of noise generation by both propeller and helicopter systems.

4.1. *The behaviour of the unsteady lift in the neighbourhood of the corner*

For simplicity we set $k_y = 0$ in (16) (so that the incident harmonic gust depends only on the chordwise coordinate x), and deform the integration contour from the real k_1'-axis onto the path which traverses the (single) branch cut in the lower half-plane; making a further simple transformation, and using the transonic similarity law (equation (5)) to extend the result to general transonic M yields

$$[p(x,y,0)]^+_- = -\frac{2V}{M^2\pi\Omega y}\exp\left(-\tfrac{1}{2}\mathrm{i}\Omega x\right)\int_0^\infty \exp\left(-\mathrm{i}\lambda u^2\right)\mathrm{erf}\left(u^{\frac{1}{2}}\right)\mathrm{d}u, \tag{17}$$

where

$$\lambda \equiv x/(2M^2\Omega y^2). \tag{18}$$

Whilst it has not proved possible to evaluate the integral in (17) in terms of well-known functions, asymptotic analysis can still be completed for λ either small or large. In the limit $\lambda \to \infty$ we find that to leading order the error function in (17) is replaced by its asymptotic form near $u = 0$ (namely, $\mathrm{erf}(u) \sim 2u/\pi^{\frac{1}{2}}$ as $u \to 0$), and it follows that

$$[p(x,y,0)]^+_- \sim -\frac{2V}{M^2\pi^{\frac{3}{2}}\Omega y}\exp\left(-\tfrac{1}{2}\mathrm{i}\Omega x\right)\frac{\exp\left(-\frac{3}{8}\pi\mathrm{i}\right)\Gamma\left(\frac{3}{4}\right)}{\lambda^{\frac{3}{4}}} \quad \text{as} \quad \lambda \to \infty. \tag{19}$$

Alternatively, when $\lambda \to 0$ we make the substitution $\lambda^{\frac{1}{2}}u = v$, and use the fact that $\mathrm{erf}(\lambda^{-\frac{1}{4}}v^{\frac{1}{2}}) \sim 1$ as $\lambda \to 0$, to show that, again to leading order,

$$[p(x,y,0)]^+_- \sim -\frac{V}{M^2\pi^{\frac{1}{2}}\Omega y}\exp\left(-\tfrac{1}{4}\pi\mathrm{i}\right)\frac{\exp\left(-\frac{1}{2}\mathrm{i}\Omega x\right)}{\lambda^{\frac{1}{2}}} \quad \text{as} \quad \lambda \to 0. \tag{20}$$

Higher-order terms in (19) and (20) could easily be calculated (indeed, the next term in (20) is found in §4.2 below), but have not been included here since they have no bearing on the structure of the corner singularity. We can now use (19) and (20) to explore the form of the lift distribution near the blade corner, and to facilitate this we define polar coordinates in the blade plane, writing $x = r\cos\Theta$ and $y = r\sin\Theta$, so that λ becomes

$$\lambda = \frac{\cos\Theta}{2M^2\Omega\sin^2\Theta}\frac{1}{r}. \tag{21}$$

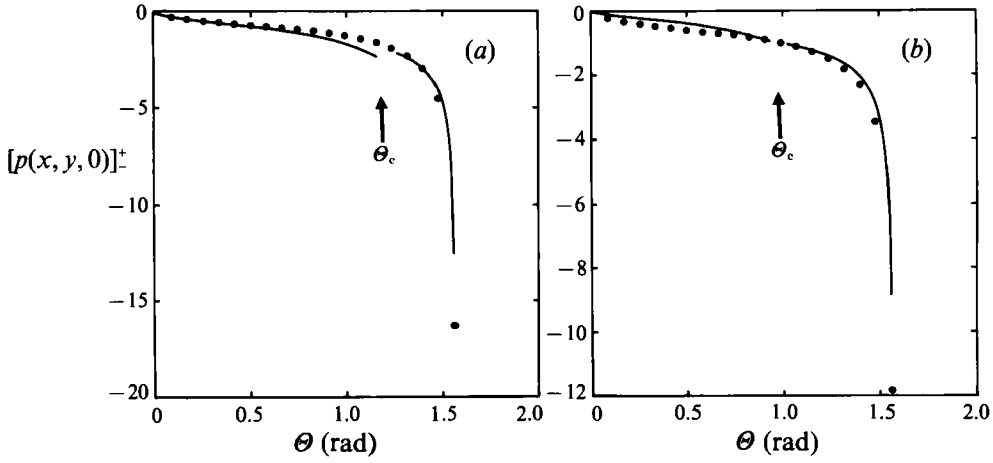

FIGURE 2. A comparison of the asymptotic approximations ((19) and (20)) to $[p(x,y,0)]^{+}_{-}$ as a function of Θ at fixed r (solid line), against an exact numerical integration of (17) (●). $k_y = 0$, $\Omega = 5$, $M = 0.9$; and (*a*) $r = 0.05$, (*b*) $r = 0.1$.

In the limit of $r \to 0$, the limiting value of λ will depend on the path along which the corner is approached; for paths lying in the wide arc for which $\cos\Theta = O(1)$ we see that $\lambda \to \infty$ as $r \to 0$, so that the asymptotic expression for the lift given in (19) must be applied; whilst for paths lying sufficiently close to the leading edge (i.e. for $\cos\Theta = o(r)$), we have $\lambda \to 0$ as $r \to 0$, and (20) must be applied. The transition between these two regions occurs across the region in which $\lambda = O(1)$, and we define a critical line, $\Theta = \Theta_c$, lying in this transition region, along which the value of λ is exactly unity; Θ_c is given by

$$\Theta_c = \cos^{-1}\left[-\frac{1}{4M^2\Omega r} + \left(\frac{1}{16M^4\Omega^2 r^2} + 1\right)^{\frac{1}{2}}\right]. \tag{22}$$

In the neighbourhood of $\Theta = \Theta_c$ no asymptotic expansion of (17) is possible, since here $\lambda = O(1)$. In order to predict the value of $[p(x,y,0)]^{+}_{-}$ for a given (small) value of r and varying Θ we therefore evaluate the outer solution by use of (19) and (20) in the ranges $0 \leqslant \Theta \leqslant \Theta_c - \delta$ and $\Theta_c + \delta \leqslant \Theta < \frac{1}{2}\pi$ respectively, where δ is a small positive constant. As already stated, the inner solution in the narrow range $\Theta_c - \delta \leqslant \Theta \leqslant \Theta_c + \delta$ cannot be calculated asymptotically and is neglected, but little information is thereby lost, and in a practical prediction scheme the two segments of the outer solution could be joined by a simple curve-fitting routine. The accuracy of our asymptotic approximations is demonstrated in figure 2 by comparison with an (exact) numerical integration of (17), for the parameters $\Omega = 5$ and $M = 0.9$, and for two different values of r ($r = 0.05$, 0.1). As can be seen, excellent agreement is obtained over most of the angular range $0 < \Theta < \frac{1}{2}\pi$, with only a very narrow region round Θ_c excluded. We note that the second term in (20) is not required to obtain good agreement with the numerical results, since in the region $\Theta > \Theta_c + \delta$ the first term in (20) is much bigger than the second for these small values of r.

Having seen how our asymptotic formulae can be applied in making a practical prediction of the lift distribution close to the blade corner, we now go on to consider the formal nature of the singularity in the lift at the blade corner. For paths along which $r \to 0$ with Θ such that both $\cos\Theta = O(1)$ and $\sin\Theta = O(1)$ (i.e. the corner is

approached on a path lying not too close to the edges of the quarter-plane), it follows from (19) that the pressure jump is singular, with

$$[p(x,y,0)]^+_- \sim r^{-\frac{1}{4}} \quad \text{as} \quad r \to 0,$$

where the coefficient of $r^{-\frac{1}{4}}$ is $O(1)$. Further consideration is required for the cases of $\cos\Theta$ or $\sin\Theta$ small, however. First, for $\cos\Theta \ll 1$ (i.e. the corner is approached along a path close to the leading edge) we write $\cos\Theta = Ar^\alpha$, with $A = O(1)$. When $0 < \alpha < 1$ we still have that $\lambda \gg 1$ near the corner, and (19) is used to demonstrate that

$$[p(x,y,0)]^+_- \sim r^{-(1+3\alpha)/4} \quad \text{as} \quad r \to 0.$$

For $\alpha = 1$ we have $\lambda = O(1)$, so that the integral in (17) is also $O(1)$, and

$$[p(x,y,0)]^+_- \sim r^{-1} \quad \text{as} \quad r \to 0;$$

the coefficient of r^{-1} is independent of r, but as stated above cannot be determined explicitly. For $\alpha > 1$ we see that $\lambda \ll 1$ near the corner, so that (20) must now be used to give

$$[p(x,y,0)]^+_- \sim r^{-(\alpha+1)/2} \quad \text{as} \quad r \to 0.$$

Second, for $\sin\theta \ll 1$ (i.e. the corner is approached along a path close to the side edge) we write $\sin\theta = Br^\beta$, with $B = O(1)$; we now have $\lambda \gg 1$ near the corner, and again applying (19) demonstrates that

$$[p(x,y,0)]^+_- \sim r^{(6\beta-1)/4} \quad \text{as} \quad r \to 0.$$

It is therefore clear that the nature of the singularity in $[p(x,y,0)]^+_-$ depends crucially on the path along which the corner is approached. For paths lying within the broad arc away from the edges $\Theta = 0$ and $\Theta = \frac{1}{2}\pi$ the pressure is singular like $r^{-\frac{1}{4}}$ at the corner. However, for paths sufficiently close to the leading edge $\Theta = \frac{1}{2}\pi$ the pressure is more singular than $r^{-\frac{1}{4}}$, and the strength of this algebraic singularity can be made arbitrarily large by choosing paths closer and closer to the leading edge (i.e. by increasing α). Close to the side edge $\Theta = 0$, however, the pressure singularity is weaker than $r^{-\frac{1}{4}}$, and indeed for paths sufficiently close to the side edge the pressure is not singular at the corner at all, but tends to zero (i.e. by choosing $\beta > \frac{1}{6}$).

It is easy to see that the right-hand side of (20) is exactly equal to the pressure distribution on an infinite-span blade (equation (A 4)), which means that for $\Theta > \Theta_c$ (which is only a narrow region for very small r) the leading term in $[p(x,y,0)]^+_-$ is unaffected by the presence of the blade corner. We therefore see that the three-dimensional effects due to the presence of the blade corner and side edge are more important in the region $\Theta < \Theta_c$, which is hardly surprising since in this region a transition must be made between the singular value of the pressure at the leading edge and its zero value at the side edge. Useful scaling laws for the dependence of the corner loading on the various operating parameters can be derived, and we note in particular from (19) and (20) that

$$[p(x,y,0)]^+_- \propto \begin{cases} \Omega^{-\frac{1}{4}} M^{-\frac{1}{2}} & \text{if} \quad \Theta < \Theta_c \\ \Omega^{-\frac{1}{2}} M^{-1} & \text{if} \quad \Theta > \Theta_c \end{cases}, \tag{23}$$

implying that, near the corner $[p(x,y,0)]^+_-$ will decrease as either M or Ω is increased.

The generalization of this analysis to include $k_y \neq 0$ could be accomplished in much the same way, but would have little bearing on the overall structure of $[p(x,y,0)]^+_-$ (the strength of the singularity for the various paths would be unaltered, and k_y would only appear in the coefficients), but this will not be attempted here.

4.2. *The behaviour of the unsteady lift distribution in the neighbourhood of the leading edge*

We now analyse the behaviour of the lift distribution close to the leading edge of the quarter-plane, considering the more general situation of the gust possessing a non-zero transverse wavenumber (i.e. $k_y \neq 0$), and rewrite (16) in the form

$$[p(x,y,0)]^{+}_{-} = -\frac{V}{(2\Omega x)^{\frac{1}{2}}M\pi}\exp(-\tfrac{1}{2}\mathrm{i}\Omega x - \mathrm{i}k_y y)\int_u \frac{\exp(-\mathrm{i}u)}{(a_2^2+u)^{\frac{1}{2}}} \times \operatorname{erf}[a_1(a_2+\mathrm{i}u^{\frac{1}{2}})^{\frac{1}{2}}\exp(-\tfrac{1}{4}\mathrm{i}\pi)]\,\mathrm{d}u, \quad (24)$$

having extended (16) to include $M \neq 1$ as before, and where the parameters a_1 and a_2 are defined by

$$a_1 \equiv (2\Omega M^2/x)^{\frac{1}{4}}y^{\frac{1}{2}} \quad (25)$$

and

$$a_2 \equiv (x/2\Omega)^{\frac{1}{2}}k_y/M. \quad (26)$$

The interpretation of the square roots in (24) follows from the definitions of the branch cuts in the original k_1- and k_2-planes.

We will determine the first two terms in the expansion of $[p(x,y,0)]^{+}_{-}$ as $x \to 0$ with y held fixed (which is equivalent to the limits $a_1 \to \infty$, $a_2 \to 0$, with $a_1^2 a_2$ constant). It is clear that these results will then give a good approximation to the lift distribution for the positions on the blade such that either x is small and $y = O(1)$, or such that both x and y are small with $x \ll y^{\frac{1}{2}}$; these correspond to positions close to the leading edge but away from the corner and to positions close to the corner but in the region $\Theta > \Theta_c + \delta$ respectively. We now rewrite (24) in the form

$$[p(x,y,0)]^{+}_{-} = -\frac{V}{(2\Omega x)^{\frac{1}{2}}M\pi}\exp(-\tfrac{1}{2}\mathrm{i}\Omega x - \mathrm{i}k_y y)\int_u \frac{\exp(-\mathrm{i}u)}{(a_2^2+u)^{\frac{1}{2}}}\mathrm{d}u + \frac{V}{(2\Omega x)^{\frac{1}{2}}M\pi}\exp(-\tfrac{1}{2}\mathrm{i}\Omega x - \mathrm{i}k_y y)\int_u \frac{\exp(-\mathrm{i}u)}{(a_2^2+u)^{\frac{1}{2}}}\operatorname{erfc}[a_1(a_2+\mathrm{i}u^{\frac{1}{2}})^{\frac{1}{2}}\exp(-\tfrac{1}{4}\mathrm{i}\pi)]\,\mathrm{d}u, \quad (27)$$

where the complementary error function $\operatorname{erfc}(z)$ is defined by

$$\operatorname{erfc}(z) \equiv 1 - \operatorname{erf}(z).$$

The leading term in the expansion of $[p(x,y,0)]^{+}_{-}$ is given by evaluating the first term in (27), and corresponds exactly to the equivalent result for the infinite-span blade found in Appendix A, which we denote as $[p_{2d}(x,y,0)]^{+}_{-}$. To determine the next term we must therefore expand the second integral in (27), and since $a_1 \to \infty$ we apply the large-argument form of $\operatorname{erfc}(z)$, i.e.

$$\operatorname{erfc}(z) \sim \frac{\exp(-z^2)}{\pi^{\frac{1}{2}}z} \quad \text{as} \quad z \to \infty, \quad (28)$$

together with the simple transformation $v = u + a_2^2$, so that the second term in (27) becomes

$$\frac{V}{M\pi^{\frac{3}{2}}(2\Omega x)^{\frac{1}{2}}a_1}\exp(-\tfrac{1}{2}\mathrm{i}\Omega x + \tfrac{1}{4}\mathrm{i}\pi - \mathrm{i}k_y y + \mathrm{i}a_1^2 a_2 + \mathrm{i}a_2^2) \times \int \frac{\exp(-\mathrm{i}v)}{v^{\frac{1}{2}}(a_2+\mathrm{i}(v-a_2)^{\frac{1}{2}})^{\frac{1}{2}}}\exp(-a_1^2(v-a_2^2)^{\frac{1}{2}})\,\mathrm{d}v. \quad (29)$$

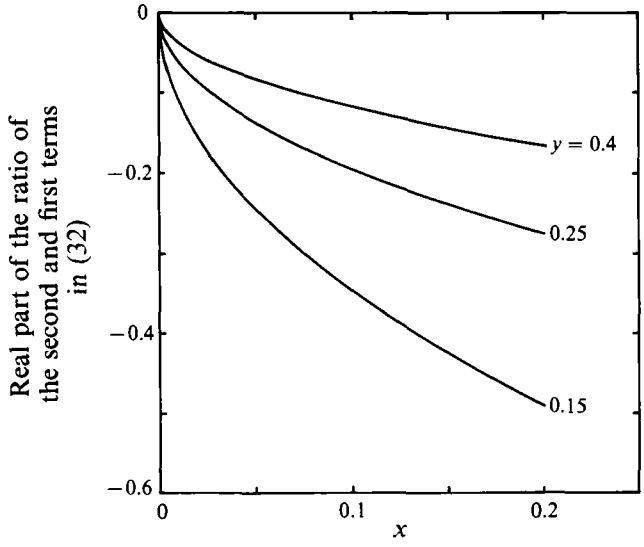

FIGURE 3. Plot of the ratio of the second and first terms in the asymptotic expansion of $[p(x,y,0)]^+_-$ for small x, with y fixed (equation (32)). $k_y = 1$, $\Omega = 5$, $M = 0.9$ and $y = 0.15, 0.25, 0.4$.

We now take the limit of $a_2 \to 0$ in the integral in (29), and deform the integration path around the branch cut (which joins $v = 0$ to infinity along the negative imaginary axis), so that after some simplification the integral in (29) becomes

$$4\exp(-\tfrac{3}{8}\pi\mathrm{i})\left\{\int_0^\infty \exp(-z^4 - a_1^2\exp[-\tfrac{1}{4}\pi\mathrm{i}]z^2)\,\mathrm{d}z - \int_0^\infty \exp(-z^4 - a_1^2\exp[-\tfrac{5}{4}\pi\mathrm{i}]z^2)\,\mathrm{d}z\right\}. \tag{30}$$

Application of the standard result (Gradshteyn & Ryzhik 1980, p. 307, 3.323(3))

$$\int_0^\infty \exp(-z^4 - a_1^2\exp[-\tfrac{1}{4}\pi\mathrm{i}]z^2)\,\mathrm{d}z = \tfrac{1}{4}K_{\frac{1}{4}}(-\tfrac{1}{8}\mathrm{i}a_1^4)\,a_1\exp(-\tfrac{1}{8}\pi\mathrm{i})\exp(-\tfrac{1}{8}\mathrm{i}a_1^4), \tag{31}$$

followed by taking the limit $a_1 \to \infty$ and applying a standard result for the large-argument form of Bessel functions of fractional order (Abramowitz & Stegun 1968, p. 378), then yields a final expression for the second term in the asymptotic expansion of $[p(x,y,0)]^+_-$, and we have that

$$[p(x,y,0)]^+_- \sim [p_{2\mathrm{d}}(x,y,0)]^+_- + \frac{2V}{M^2\pi y\Omega}\exp(-\tfrac{1}{2}\mathrm{i}\Omega x - \mathrm{i}k_y y + \mathrm{i}a_1^2 a_2 + \mathrm{i}a_2^2) + O(x^{\frac{1}{2}}). \tag{32}$$

We therefore see that the effects of the corner and side edge arise only in the second (and higher) terms in the expansion of the lift distribution. The ratio of this second term to the first is plotted in figure 3, and it is clear that the second term can become significant, even for the relativity small values of x considered here. The magnitude of the second term decreases with increasing y, indicating that for small x the effects of the corner becomes negligible at sufficiently large distance along the blade span. In fact, we can prove that this is the case for all x by consideration of (24); in the limit of $y \to \infty$, with x held fixed, the error function factor in (24) can be replaced by its large-argument value of unity, and the subsequent integral then evaluated to give

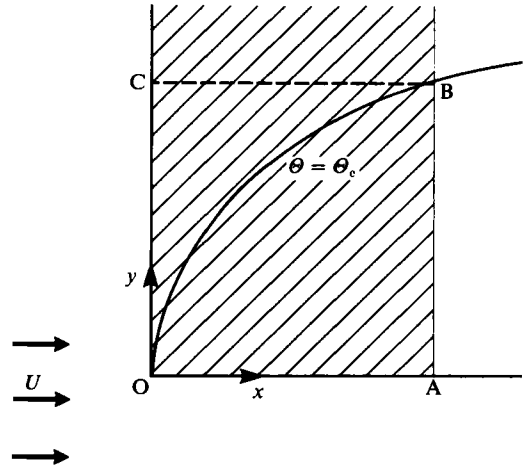

FIGURE 4. The structure of the unsteady lift distribution; the hatched region corresponds to a strip of width $O(\Omega)^{-1}$ along the blade leading edge.

exactly the two-dimensional result found in Appendix A. Sufficiently far from the side edge our quarter-plane problem therefore reduces precisely to consideration of an infinite-span blade.

4.3. *The lift distribution throughout a strip of width* $O(\Omega)^{-1}$

Following the analysis of §§4.1 and 4.2 above, the general structure of the unsteady lift distribution is described in figure 4. We consider the strip bounded by the leading edge on one side, and the parallel line through the points A and B on the other (i.e. the hatched region in the figure); the distance between the corner, O, and A is $O(\Omega)^{-1}$. The line $\Theta = \Theta_c$ (i.e. $y^2 = x/2M^2\Omega$, from (18)) intersects this second line at B, and it is clear that the distance OC is also $O(\Omega)^{-1}$. In the region OAB we have that $[p(x, y, 0)]^{+}_{-}$ is given by (20), whilst in the remainder of the shaded region it is given by (32). In the region OBC, but close to the corner, the second term in (32) will be very much smaller than the first (since here we have that x is very small, so that the leading-edge singularity contained in the first term dominates the finite second term), and could be neglected; this is the reason why the asymptotic results plotted in figure 2 (which were in part based on (20), which contains only the first term of (32)) agreed closely with the numerical results. In contrast, the results plotted in figure 3 correspond to positions on the blade span lying in the hatched region of figure 4 but in the neighbourhood of, or above, the line BC, and it is clear that here this second term cannot be neglected. That our asymptotic results from §§4.1 and 4.2 should be valid in these various regions follows from the fact that Ω^{-1} is a small parameter, so that A and B are indeed close to the corner and side edge, allowing application of our small-r and small-x asymptotic limits. Matching of the expressions across the boundary OB, in the strict sense of matched asymptotic theory, cannot be completed, since no asymptotic analysis of (17) can be performed for the parameter $\lambda = O(1)$.

In summary, we have therefore constructed asymptotic expressions for the lift distribution throughout a strip of width $O(\Omega)^{-1}$ along the leading edge, and it is again emphasized that it is this portion of the blade which is most significant in terms of noise generation; what we have essentially done is to specify the equivalent dipole

distribution along the leading edge. A further possible practical application of these results might be as a means of testing the accuracy of the CFD-type codes currently being developed for the prediction of propeller or helicopter blade–vortex interaction noise.

5. The acoustically weighted lift

As was seen in the previous section, it has not proved possible to evaluate the integral representation of the detailed lift distribution (e.g. (17)) in terms of well-known functions, and progress could only be made by application of asymptotic analysis close to the leading edge and corner of the blade. However, an exact closed-form expression for the chordwise integral of the lift can be derived, and in this section we therefore consider the acoustically weighted lift for the quarter-plane, $\mathscr{L}(y,K)$, defined by

$$\mathscr{L}(y,K) \equiv \int_0^\infty [p(x,y,0)]_-^+ \exp(-\mathrm{i}Kx)\,\mathrm{d}x. \tag{33}$$

This quantity will be significant in the prediction of propfan noise; essentially $\mathscr{L}(y,K)$ is the effective unsteady lift which acts to produce sound, where K is a wavenumber which accounts for retarded-time differences along the blade chord and depends on the various propfan operating parameters. Of course, the acoustically weighted lift on a real propeller blade (denoted $\Psi(y,K)$ and given in (B 2)) would be somewhat different from (33), due to the presence of the trailing edge; for a real blade the range of integration in the acoustically weighted lift would be between 0 and 1, and $[p(x,y,0)]_-^+$ would include the effects of the trailing edge. However, (33) can still be applied in practice, thanks to the fact that the blade number, B, is large in modern systems, permitting application of the asymptotic limit $B \to \infty$ (this has already been used extensively in propfan noise prediction – see Peake & Crighton 1991). We have that $K \propto B$ (equation (B 3)), so that in the large-blade-number limit $K \to \infty$, allowing the trailing edge to be neglected and the chordwise integration to be extended to infinity. In this limit the acoustically weighted lift on a real propeller blade therefore approximates to the acoustically weighted lift on our quarter-plane (i.e. $\Psi(y,K) \sim \mathscr{L}(y,K)$), and full details are given in Appendix B. When $K = 0$, the quantity $\mathscr{L}(y,K)$ reduces to the ordinary lift per unit span.

We write $\mathscr{L}(y,K)$ in terms of the Fourier inversion integral of $[p(x,y,0)]_-^+$, so that

$$\mathscr{L}(y,K) = \frac{1}{4\pi^2}\int_{-\infty}^{\infty}\int_{k_1}\int_{k_2} [P(k_1,k_2,0)]_-^+ \exp(-\mathrm{i}Kx - \mathrm{i}k_1 x - \mathrm{i}k_2 y)\,\mathrm{d}k_2\,\mathrm{d}k_1\,\mathrm{d}x; \tag{34}$$

the fact that $[p(x,y,0)]_-^+$ vanishes upstream of the leading edge has allowed the lower limit of integration in (33) to be replaced by $-\infty$. Exchanging the orders of integration in (34), evaluating the x-integral as $2\pi\delta(k_1+K)$, substituting for $[P(k_1,k_2,0)]_-^+$ from (13) and completing the resulting integral in much the same way as in the derivation of (16) leads to an expression for $\mathscr{L}(y,K)$ in the case $M = 1$, and by application of the transonic similarity law (5) we find that for general values of M in the transonic range

$$\mathscr{L}(y,K) = \frac{2\mathrm{i}V}{(M^2\Omega^2 - k_y^2 + 2M^2\Omega K)^{\frac{1}{2}}} \exp(-\mathrm{i}yk_y)\,\mathrm{erf}[y^{\frac{1}{2}}\exp(\tfrac{1}{4}\mathrm{i}\pi)\,(M(\Omega^2+2\Omega K)^{\frac{1}{2}} - k_y)^{\frac{1}{2}}]. \tag{35}$$

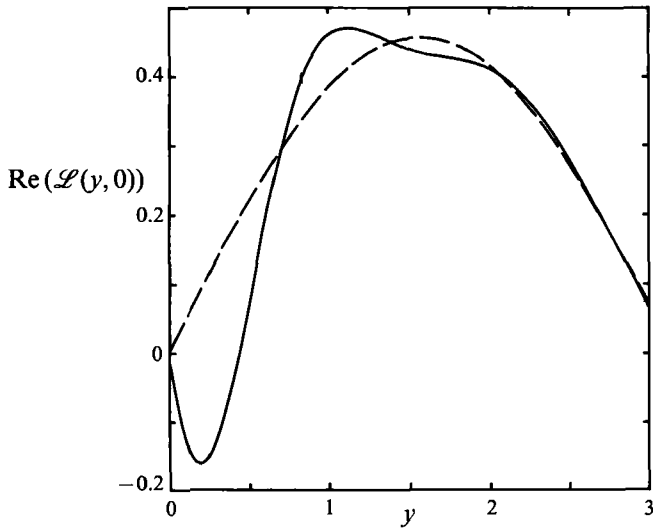

FIGURE 5. A plot of the real part of the acoustically weighted lift for the quarter-plane, $\mathscr{L}(y,K)$ (solid line) and of an infinite-span blade, $\mathscr{L}_{2d}(y,K)$ (dashed line) against y; $k_y = 1$, $\Omega = 5$, $M = 0.9$ and $K = 0$.

In appendix A the corresponding result for an infinite-span (two-dimensional) blade (denoted $\mathscr{L}_{2d}(y,K)$) is shown to correspond exactly to the expression given in (35), but without the error-function factor. We therefore see that the effects of the corner on $\mathscr{L}(y,K)$ occur only in the error function; the magnitude of these effects is given by the so-called *three-dimensional flow correction coefficient*, C (Landahl 1989), defined by

$$C \equiv [\mathscr{L}(y) - \mathscr{L}_{2d}(y)]/\mathscr{L}_{2d}(y),$$

which becomes

$$C = -\operatorname{erfc}[y^{\frac{1}{2}} \exp(\tfrac{1}{4}i\pi)(M(\Omega^2 + 2\Omega K)^{\frac{1}{2}} - k_y)^{\frac{1}{2}}]. \tag{36}$$

We note that C approaches zero (i.e. the two-dimensional result for the lift distribution is regained) in the limit of the argument of the complementary error function in (36) approaching infinity, and this has a number of implications. First, we have that far from the corner (i.e. as $y \to \infty$) the effects of the corner become negligible, in agreement with the result of the previous section. Second, for very large reduced frequencies, or large values of the wavenumber K, the acoustically weighted lift distribution is close to the two-dimensional, infinite-span result along most of the blade span, apart from very close to the side edge (i.e. $y \approx 0$). Third, we see that the level of the corner effect decreases with increasing M. These trends with Ω and M are in agreement with the results found for the scaling of the lift distribution near the corner (equation (23)). In figure 5, $\mathscr{L}(y,0)$ and $\mathscr{L}_{2d}(y,0)$ are plotted against y for $M = 0.9$, $\Omega = 5$; the two curves are seen to agree for distances from the corner of about 1.5 chord lengths or greater, but vary markedly closer to the corner. Since modern propellers will have relatively long blade chords (typically 0.3 of a blade radius), and since, as argued in the introduction, the corner region is the most important portion of the rear-row blades for noise generation, it can be seen from figure 5 that the two-dimensional theory presented in appendix A will not be an adequate basis for the prediction of wake or tip-vortex interaction noise. The three-dimensional flow correction coefficient is plotted in figure 6 for $M = 0.9$, 1, 1.1,

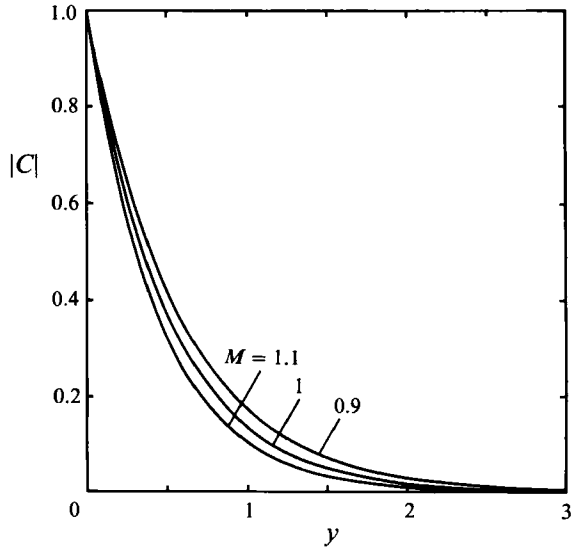

FIGURE 6. A plot of the absolute value of the three-dimensional flow correction coefficient, C, against y, for $k_y = 1$, $\Omega = 5$ and for $M = 0.9$, 1, 1.1.

demonstrating the reduction in the effect of the corner as M is increased within the transonic range.

In summary, we have therefore presented in this section a simple algebraic result for C, which can be easily incorporated into existing propeller noise prediction schemes in order to correct two-dimensional response calculations for the presence of the blade corner.

6. The radiation

In the previous two sections we considered the lift distribution on the quarter-plane, and the results obtained had a number of practical applications, either in the direct prediction of the gust loading on a rectangular surface in rectilinear motion (e.g. a wing), or in determining the radiation produced by the unsteady loading on a rotating propfan blade, using the method outlined in Appendix B. In this section we now consider the far-field form of the unsteady pressure generated by the interaction between the gust and the quarter-plane, and whilst, as has already been argued, these results will not be applicable in the propfan or helicopter cases (since far from a rotating blade the approximation of rectilinear motion becomes invalid), they will be applicable to the question of noise generation by a gust–wing interaction. The radiation has previously been considered by Cargill (1987).

We start from the exact double-integral expression

$$p(x,y,z) = \mp \frac{\mathrm{i}V}{4\pi^2 M} \int\int \frac{\exp\left(-\mathrm{i}|\boldsymbol{x}|\,\psi(k_1,k_2)\right)\mathrm{d}k_1\,\mathrm{d}k_2}{\gamma^+(k_1,k_2)\,\gamma^-(k_1,k_y/M)\,(k_2-k_y/M)}, \tag{37}$$

which is simply derived by applying the similarity law (5) to (15) and using the usual potential theory relation between the pressure and the potential. In (37), $|\boldsymbol{x}|$ is the observer–corner separation, and the phase function $|\boldsymbol{x}|\,\psi(k_1,k_2)$ is defined by

$$|\boldsymbol{x}|\,\psi(k_1,k_2) \equiv k_1 x + Mk_2 y - \mathrm{i}M\gamma(k_1,k_2)\,|z|. \tag{38}$$

Since we shall subsequently be applying asymptotic analysis in the limit $|\boldsymbol{x}| \to \infty$, we first note that the argument of the exponential in (37) possesses a single stationary phase point, i.e. the point $k_1 = \tilde{k}_1$, $k_2 = \tilde{k}_2$ which satisfies

$$\frac{\partial \psi(\tilde{k}_1, \tilde{k}_2)}{\partial k_1} = \frac{\partial \psi(\tilde{k}_1, \tilde{k}_2)}{\partial k_2} = 0,$$

and we find that

$$\tilde{k}_1 = \tfrac{1}{2}\Omega\left\{1 - \frac{M^2(y^2+z^2)}{x^2}\right\}, \quad \tilde{k}_2 = \frac{M\Omega y}{x}, \tag{39}$$

and

$$\gamma(\tilde{k}_1, \tilde{k}_2) = \mathrm{i}M|z|\,\Omega/x. \tag{40}$$

It is easy to check that the values of $\gamma(\tilde{k}_1, \tilde{k}_2)$ given in (40) lies on the correct Riemann sheet. A further step in the analysis will be the calculation of the determinant of the Hessian matrix, $\mathscr{H}(k_1, k_2)$, of second partial derivatives of $\psi(k_1, k_2)$, i.e.

$$\mathscr{H} \equiv \frac{\partial^2 \psi}{\partial k_i \partial k_j},$$

and we find that

$$\det \mathscr{H}(\tilde{k}_1, \tilde{k}_2) = x^4/(z^2 M^2 \Omega^2 |\boldsymbol{x}|^2), \tag{41}$$

and that the signature of $\mathscr{H}(\tilde{k}_1, \tilde{k}_2)$ is -2.

For $x < 0$ the k_1 integral is completed by closing the k_1 contour in the upper half-plane, and since the integrand is analytic there we have that $p(x, y, z) = 0$ for $x < 0$. In order to find the far-field form of $p(x, y, z)$ in $x > 0$ we now take the limit $|\boldsymbol{x}| \to \infty$, and note that in this limit there will be a dominant contribution to the integral in (37) from the neighbourhood of the stationary phase point $k_1 = \tilde{k}_1$, $k_2 = \tilde{k}_2$. From (40) we see that $\gamma(k_1, k_2)$ is purely imaginary in the neighbourhood of the stationary phase point, and that the phase function in (38) is therefore in exactly the right form for application of the method of stationary phase for double integrals (that is to say, the phase function is equal to the large parameter multiplied by a real number), as described by Jones (1966). As part of this method, the integration contours in both the k_1- and k_2-planes must be deformed from the real axis onto straight lines through $k_1 = \tilde{k}_1$ and $k_2 = \tilde{k}_2$ respectively, with both of these lines at an angle of $\frac{1}{4}\pi$ to the respective real axes, and as a result of this deformation there is therefore the possibility of a contribution to $p(x, y, z)$ from the pole at $k_2 = k_y/M$, in addition to the contribution from the stationary phase point. The contribution to $p(x, y, z)$ from this pole (which we shall denote $p_{2\mathrm{d}}(x, y, z)$, for reasons which will become clear) arises only if the pole is to the left of the point $k_2 = \tilde{k}_2$ in the k_2-plane, i.e. only if $\tilde{k}_2 > k_y/M$, and is found by application of the residue theorem to the k_2 integral in (37), leaving a single integral in the k_1-plane, which can easily be evaluated to give

$$p_{2\mathrm{d}}(x, y, z) = \mp \frac{V}{(2M^2\Omega\pi x)^{\frac{1}{2}}} \exp\left(-\tfrac{1}{4}\mathrm{i}\pi - \tfrac{1}{2}\mathrm{i}\Omega x - \mathrm{i}\frac{M^2\Omega z^2}{2x} + \mathrm{i}\frac{x k_y^2}{2\Omega M^2} - \mathrm{i}k_y y\right) \mathrm{H}\left(y - \frac{x k_y}{M^2\Omega}\right), \tag{42}$$

where $\mathrm{H}(y)$ is the unit step function. The expression given in (42) is seen to correspond to a two-dimensional radiation field, since it possesses an inverse square root fall-off with distance and its directivity is independent of the transverse coordinate y. Indeed, putting aside the step function factor, (42) is exactly equal to the radiation produced by an infinite-span blade (equation (A 7)), and we therefore see that $p_{2\mathrm{d}}(x, y, z)$ is generated by the interaction of the gust with the leading edge,

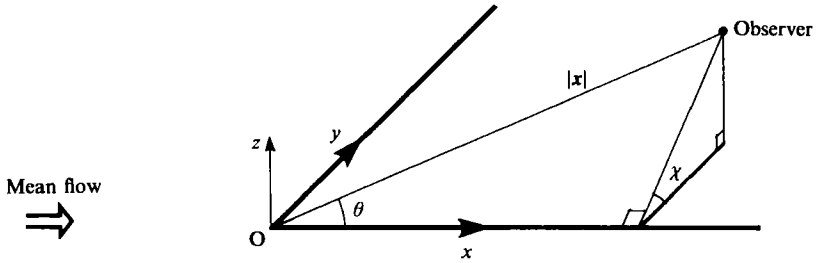

FIGURE 7. Definition of the spherical polar coordinates used in determining the far-field radiation.

and that the presence of $p_{2d}(x,y,z)$ in our problem is a result of the quarter-plane being infinite in the positive y-direction. It follows from (39) that this two-dimensional field is 'cut on' across the critical plane $y = x\tan\Lambda/M^2$, where Λ is the gust phase angle, defined by $\tan\Lambda = k_y/\Omega$. In the case of $M = 1$ the angle between this critical plane and the leading edge (i.e. $\frac{1}{2}\pi - \Lambda$) is the same as the angle between the gust phase fronts and the leading edge, and this is exactly as one might expect, since $p_{2d}(x,y,z)$ arises purely from the interaction between the gust and the leading edge (and not the corner or side edge, the effects of which are restricted to the term $p_{3d}(x,y,z)$ found below). For $M \neq 1$ in the transonic range we see that the angle of this critical plane to the leading edge is modified – the extent of the region over which $p_{2d}(x,y,0)$ is cut on increases as M is increased.

The contribution to $p(x,y,z)$ from the stationary phase point (which we denote as $p_{3d}(x,y,z)$) is now given by the standard stationary-phase formula (Jones 1966, p. 345), and defining spherical polar coordinates centred on the blade corner and given by $x = |\boldsymbol{x}|\cos\theta$, $y = |\boldsymbol{x}|\sin\theta\cos\chi$ and $z = |\boldsymbol{x}|\sin\theta\sin\chi$ (see figure 7), we find that

$$p_{3d}(x,y,z) = \pm\frac{VM\Omega^{\frac{1}{2}}(\sin\theta)^{\frac{1}{2}}\sin\chi}{2\pi\mathrm{i}\,|\boldsymbol{x}|(1-\cos\chi)^{\frac{1}{2}}(k_y\cos\theta + M^2\Omega\sin\theta)^{\frac{1}{2}}} \times \frac{1}{M^2\Omega\sin\theta\cos\chi - k_y\cos\theta}\exp\left(-\mathrm{i}\frac{\Omega|\boldsymbol{x}|}{2\cos\theta}[\cos^2\theta + M^2\sin^2\theta]\right). \quad (43)$$

Equation (43) represents a fully three-dimensional radiation field, since it possesses an $|\boldsymbol{x}|^{-1}$ fall-off with distance, and a directivity which depends on both polar angles θ and χ. We note that $p_{3d}(x,y,z)$ is in fact singular for observer positions satisfying $M^2\Omega\sin\theta\cos\chi = k_y\cos\theta$ (i.e. on the critical plane along which the pole contribution $p_{2d}(x,y,z)$ is cut on). This non-uniformity in our asymptotic expansion is due to the coincidence of the stationary phase point at $k_2 = \tilde{k}_2$ and the pole at $k_2 = k_y$; a uniform expansion of the stationary phase contribution in terms of a complex error function is of course possible, and combines with the discontinuous $p_{2d}(x,y,z)$ to yield a total pressure (i.e. $p_{2d}(x,y,z) + p_{3d}(x,y,z)$) which is continuous across the critical plane. This feature is an exact parallel to the occurrence of a shadow boundary in the two-dimensional Sommerfeld diffraction problem of scattering by an edge (see Jones 1986), but the detailed mathematics will not be presented here. We also note that (43) becomes invalid in the Mach wave direction, $\cos\theta = 0$, since in the limit $\theta \to \frac{1}{2}\pi$ the stationary phase point approaches infinity and the method of stationary phase breaks down. In the limit $\chi \to 0$ (i.e. as the quarter-plane surface is approached), $p_{3d}(x,y,z)$ approaches a finite non-zero value, corresponding to the component of the surface pressure distribution resulting from the gust–corner interaction.

In summary we therefore see that, downstream of $\theta = \frac{1}{2}\pi$, the radiated field

comprises two components, which must be added to find the total pressure $p(x, y, z)$ around the quarter-plane. First, there is the two-dimensional field $p_{2d}(x, y, z)$, which is non-zero in the range $y > x \tan \Lambda/M^2$, and arises from the interaction between the gust and the semi-infinite leading edge; in fact, for a realistic wing with a finite span, $p_{2d}(x, y, z)$ would not be present in this form. The role of the blade corner in determining $p_{2d}(x, y, z)$ is merely in fixing the position of the critical plane across which $p_{2d}(x, y, z)$ is cut on, but otherwise has no bearing on the magnitude of $p_{2d}(x, y, z)$. Second, we have the fully three-dimensional field $p_{3d}(x, y, z)$, which is non-zero throughout the region $0 \leqslant \theta < \frac{1}{2}\pi$, and arises as a result of the presence of the corner. In this paper we are primarily interested in the effects of the corner in the conversion of incident vortical energy into acoustic energy, and since this process is described purely by $p_{3d}(x, y, z)$, it will be the acoustic intensity associated solely with this term which will give a measure of the energy scattered by the corner; this quantity will be calculated later.

We might have expected that in our quarter-plane problem the existence of a Mach surface in the flow would depend on the value of the free-stream Mach number, M; if $M < 1$ then no such surface would be present (since the governing equations would then be elliptic) and the solution for the scattered potential would be non-zero through all space; whilst for $M \geqslant 1$ a Mach surface would be present, at an angle of inclination of less than or equal to $\frac{1}{2}\pi$ to the flow direction (with equality in the $M = 1$ case), and that upstream of this surface the solution would vanish. However, since the transonic similarity law (equation (5)) states that solutions of (4) for $M \neq 1$ in the transonic range are related to the $M = 1$ solution essentially by rescaling the y- and z-coordinates (which of course has no effect on the existence or position of the Mach surface), we note that our solution for $\phi(x, y, z)$ possesses a Mach surface with inclination $\frac{1}{2}\pi$ for each value of M in the transonic range (i.e. for values of M greater than and less than unity). This feature of our solution does not in fact contradict the above arguments, however, since the expression we have derived for $\phi(x, y, z)$ is only the leading term in a series expansion of the exact unsteady potential, the higher-order terms of which are at least $O(1-M)$ smaller than this first term (equation (4) ff). For $M < 1$ this means that, since our first term is zero for $x < 0$, the exact field upstream of the corner must be given purely by these undetermined higher-order terms; the total upstream scattered field is therefore at least $O(1-M)$ smaller than the downstream part of the first term found in this paper. This is exactly as might be expected, since for high subsonic Mach numbers only a small amount of upstream influence is possible, and would vanish in the limit $M \to 1-$. For $M > 1$ in the transonic regime our analysis predicts that the orientation of the Mach surface is modified from its $M = 1$ value by only a small amount, and that this modification must again be accounted for purely by the undetermined higher-order terms. The expressions for the unsteady potential developed in this paper are therefore a good first approximation throughout the fluid, and for each M in our transonic range.

In assessing the effect of the gust–corner interaction on the radiation in this rectilinear-motion problem it is useful to consider the transport of energy to the far field, and in particular to calculate the acoustic intensity, I. We follow Goldstein (1976), who defines the intensity vector corresponding to some perturbation to a uniform mean flow as

$$\boldsymbol{I} \equiv \left(\frac{p'}{\rho_0} + \boldsymbol{U}\cdot\boldsymbol{u}'\right)(\rho_0 \boldsymbol{u}' + \rho' \boldsymbol{U}), \tag{44}$$

where $\boldsymbol{U}$ and ρ_0 are the uniform undisturbed velocity and density, and $\boldsymbol{u}'$, p' and ρ'

are the perturbation velocity, pressure and density respectively. Since we are only interested in the effects of the presence of the corner and side edge on the interaction, we shall consider the acoustic intensity due solely to the three-dimensional field $p_{3d}(x, y, z)$. Moreover, we calculate only the radial component of $\boldsymbol{I}$ (denoted I_r), since this is what is required in determining the total integrated energy flux (i.e. the energy flux integrated over a large sphere centred at the origin) in our blade-fixed reference frame. We therefore have from (44) that (in non-dimensionalized units)

$$I_r = -\mathrm{i}\Omega\phi_{3d}\left(\frac{\partial\phi_{3d}}{\partial r}+M^2\cos\theta p_{3d}\right), \tag{45}$$

and inserting the far-field expression for $\phi_{3d}(x, y, z)$ (which is easily derived in terms of $p_{3d}(x, y, z)$ from (15)), we find that

$$\overline{I_r} \sim \frac{(M^2+1)\cos\theta}{1+M^2\tan^2\theta}|p_{3d}(x, y, z)|^2, \tag{46}$$

where the overbar denotes that the intensity has been time-averaged. For simplicity we consider $k_y = 0$, in which case (46) reduces to

$$\overline{I_r} \sim \frac{V^2}{4\pi|x|^2\Omega^2}\frac{(1+M^2)\cot^2\theta\cos\theta}{M^4(\cos^2\theta+M^2\sin^2\theta)}\frac{\tan^2\chi}{1-\cos\chi}. \tag{47}$$

Clearly, the total radiation intensity (i.e. the intensity obtained from substituting the sum of p_{2d} and p_{3d}, and the corresponding velocities, into (44)) will include contributions from both the leading edge (two-dimensional) and corner (three-dimensional) fields individually, as well as a cross-term; the result given in (47) will of course agree with this total intensity in regions of space for which $p_{2d}(x, y, z) = 0$ (so that from (42), equation (47) gives the total radiation intensity for observer positions satisfying $y < xk_y/(M^2\Omega)$). We note, however, that the integral of the total energy intensity over a sphere at infinity does not converge (since $p_{2d}(x, y, z)$ decays only cylindrically at infinity), essentially due to the presence of a semi-infinite leading edge in our model; for this reason we restrict attention to our expression (47) for the intensity due solely to the three-dimensional field, which as already argued gives an indication of the level of the corner effects.

Equation (47) can now be used to analyse the angular dependence of $\overline{I_r}$, although we note that it will not be valid in the vicinity of the critical plane across which $p_{2d}(x, y, z)$ is cut on (given our choice $k_y = 0$ this plane corresponds to $\sin\theta\cos\chi = 0$, i.e. $y = 0$). If we fix θ and $|x|$ and vary χ (that is, move on a single circular section of the cone with semi-vertical angle θ and axis of symmetry aligned along the x-axis) we see that the variation in $\overline{I_r}$ is given by the factor

$$D(\chi) = \tan^2\chi/(1-\cos\chi). \tag{48}$$

The quantity $D(\chi)$ is plotted in figure 8 (our expansion of $D(\chi)$ breaks down close to the critical plane, correspondingly to $\chi = \frac{1}{2}\pi$ and $\chi = \frac{3}{2}\pi$); however, it can still be seen that the largest acoustic intensity from the corner interaction is beamed in directions directly above (and below) the blade, which is hardly surprising since the radiation is being generated by an unsteady force which acts normal to the blade. There is a null in $\overline{I_r}$ in the direction $\chi = \pi$, so that the gust–corner interaction has negligible effect in the region close to the plane $z = 0$ and outboard of the blade tip (i.e. for $y < 0$). Alternatively, $\overline{I_r}$ has a minimum in the $z = 0$ plane inboard of the tip (i.e. for

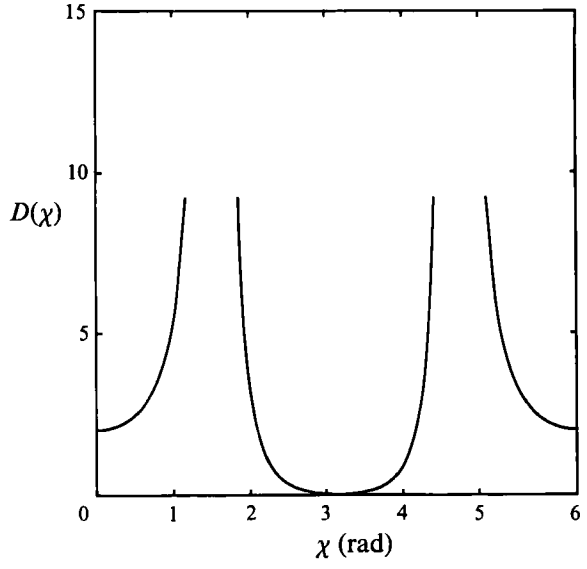

FIGURE 8. A plot of the quantity $D(\chi)$ against χ.

$y > 0$); this minimum is non-zero because the rigid quarter-plane supports a non-zero surface pressure. The variation of $\overline{I}_r$ with θ and M is determined by the factor

$$E(\theta,M) = \frac{(1+M^2)\cos\theta}{M^4(1+M^2\tan^2\theta)\sin^2\theta}, \tag{49}$$

and this time our expansion of $E(\theta,M)$ is invalid in the vicinity of $\theta = 0$ (i.e. close to the x-axis). The most significant point to note from (49), however, is that the non-uniformity along the Mach surface ($\theta = \frac{1}{2}\pi$), which was present in our expression for $\underline{p}_{3d}(x,y,z)$ due to the proximity of the wave front, has been removed, and indeed that $\overline{I}_r \to 0$ as $\theta \to \frac{1}{2}\pi$. This is exactly as one might expect, since all the acoustic energy will be convected downstream by the transonic mean flow, so that the intensity measured by an observer fixed directly above or below the corner is zero. It can also be seen from (49) that $\overline{I}_r$ is a decreasing function of M, for any θ, and therefore that the total energy generated purely by the gust–corner interaction and subsequently reaching the far field in the form of acoustic radiation must also decrease as M is increased within the transonic range. Finally, we note from (47) that $\overline{I}_r \propto \Omega^{-2}$, so that the energy radiated from the gust–corner interaction must decrease as the reduced frequency is increased. These deductions that the strength of the gust–corner interaction decreases with increasing M and Ω are fully in agreement with the trends determined by consideration of the lift distribution in §§4, 5.

7. Strip-theory approximation

A common practical technique in estimating the radiation generated by unsteady gust loading on a wing is the use of a *strip-theory* approximation, whereby the wing is divided into thin (effectively two-dimensional) strips aligned parallel to the mean flow direction. The lift distribution on each strip is then approximated by supposing that it is exactly equal to that found on a wing of infinite span, thereby neglecting the influence of the wing tip on the surface pressure. The noise can then be estimated by the use of standard radiation integrals.

Although in practice one would be seeking to apply the strip-theory method in complicated situations (perhaps including blade thickness, finite chord or non-zero incidence effects), the simple quarter-plane problem discussed in this paper can be used as a bench-mark test; following Cargill (1987), all that needs to be done is to compare the approximate prediction of the quarter-plane radiation made using strip theory with the exact results found in §6. The strip-theory approximation is that the lift distribution on our semi-infinite wing is given by (A 4) for $y \geqslant 0$, and is equal to zero for $y < 0$ (i.e. the surface pressure on our quarter plane is supposed equal to that on an infinite-span wing). The Fourier transform of this approximation to the surface pressure is denoted by $P_{\mathrm{st}}(k_1, k_2, 0)$, and it can be shown that it is related to the exact result found earlier (see (13)) by

$$\frac{P_{\mathrm{st}}(k_1, k_2, 0)}{P(k_1, k_2, 0)} = \frac{\gamma^+(k_1, k_2)}{\gamma^+(k_1, k_y)}, \tag{50}$$

as is done by Cargill (1987). Evaluation of the far-field form of the pressure predicted by strip theory follows from the method of stationary phase in exactly the same way as described in §6; the two-dimensional part of the pressure, arising from the pole contribution from $k_2 = k_y$, is precisely as before (since the right-hand side of (50) is unity when $k_2 = k_y$); whilst the stationary phase contribution is equal to the exact result (43) multiplied by the factor

$$\frac{\gamma^+(\tilde{k}_1, \tilde{k}_2)}{\gamma^+(\tilde{k}_1, k_y/M)} = M\left(\frac{1-\cos\chi}{M^2-(k_y/\Omega)\cot\theta}\right)^{\frac{1}{2}}. \tag{51}$$

In order for the strip theory to yield a good approximation for the noise, we require that the factor given in (51) be close to unity, and therefore that both θ and χ be close to $\frac{1}{2}\pi$. Hence, we see that for our quarter-plane problem the strip-theory approach will only yield an accurate result for observer positions lying close to the z-axis (i.e. directly above or below the corner). Away from the z-axis there is an error in the directivity, the magnitude of which becomes particularly large close to the plane on which the denominator of (51) vanishes. Thus, whilst the strip theory does not produce an accurate prediction of the radiation in this problem over most of the angular range, we see that the resulting strip-theory approximation can easily be modified by inclusion of the simple multiplicative factor given in (51). There is therefore the possibility of using this factor as a *tip correction coefficient* in a practical wing-loading noise prediction scheme; features such as finite chord, thickness or mean loading would be accounted for in the lift distribution using strip theory, and, as a first approximation, the resulting radiation corrected to account for the presence of the wing tip by inclusion of our simple factor.

8. Concluding remarks

In this paper the unsteady interaction between a harmonic velocity gust and a quarter-plane in transonic flow has been investigated, and application of a transonic similarity law has allowed us to derive a solution which is correct to leading order in the small parameter $(1-M)$. The nature of the singularity in the lift distribution at the blade corner was analysed, and it was shown that, unusually, the strength of the singularity depended crucially on the path along which the corner was approached. The detailed lift distribution in a strip of width $O(\Omega)^{-1}$ about the leading edge was found, and was seen to be divided into two regions – one in which the leading-edge

inverse-square-root singularity dominates, and the other in which the transition is made between this singularity and the zero value in the lift at the side edge. In terms of propfan noise prediction, the quantity of most practical interest is the acoustically weighted lift, and an exact algebraic expression for this in our quarter-plane problem was derived, and was seen to be equal to the equivalent result for a realistic finite-chord blade in the asymptotic limit of large blade number. This analysis yielded a simple algebraic factor, which could easily be included in prediction schemes in order to correct for the effects of the rear-row blade tips on the interaction noise.

In addition to consideration of the lift distribution, the radiation in the quarter-plane problem was also discussed. Far from the corner the scattered field was seen to be composed of two components; one (two-dimensional) term arising from the interaction between the gust and the semi-infinite blade leading edge; and a second (genuinely three-dimensional) term corresponding to the interaction of the gust with the corner and side edge. It was this second term which was of greater interest, since it represented the effect of the gust–corner interaction at infinity, and expressions for the directivity and scaling of the acoustic intensity were derived. The accuracy of the strip-theory approximation for radiation prediction in this simple model problem was also assessed.

The advantage of the approach described in this paper over a numerical integration of the governing equations has been that closed-form algebraic expressions for various significant quantities have been derived, in the practically important transonic flow regime. The analysis has yielded physical insight into the structure of the scattered field and the nature of unsteady corner interactions, and has provided approximate formulae and scaling laws which should be of practical interest.

The author is particularly grateful to A. M. Cargill for suggesting this problem, and for the financial support provided by Emmanuel College, Cambridge.

Appendix A

In this appendix we present the results for the lift distribution and radiation generated by the interaction between the harmonic gust and the infinite-span blade $\{x > 0,\ -\infty < y < \infty,\ z = 0\}$; recall that the semi-infinite blade, or quarter-plane, considered in this paper occupies the quadrant $\{x > 0,\ 0 \leqslant y < \infty,\ z = 0\}$. The analysis proceeds in much the same way as before; since the problem is essentially two-dimensional in nature, the transverse, y, dependence of the scattered potential must be equal to that of the incident gust, so that the scattered potential is written in the form $\psi(x,y)\exp(-\mathrm{i}k_y y - \epsilon y)\exp(\mathrm{i}\Omega t)$. Substituting this into the small-disturbance equation (4) yields

$$\psi_{zz} - 2\mathrm{i}M^2\Omega\psi_x + (M^2\Omega^2 - (k_y - \mathrm{i}\epsilon)^2)\psi = 0, \tag{A 1}$$

and $\psi(x,z)$ is in addition subject to the boundary conditions

$$\psi_z(x,0) + V\exp(-\mathrm{i}\Omega x) = 0 \quad \text{for} \quad x > 0$$

and

$$\psi(x,0) = 0 \quad \text{for} \quad x < 0.$$

Defining the one-dimensional Fourier transform

$$\Psi(k,z) = \int_{-\infty}^{\infty} \exp(\mathrm{i}kx)\,\psi(x,z)\,\mathrm{d}x, \tag{A 2}$$

we find by application of the Wiener–Hopf technique (this time with respect to the k transform variable), that the Fourier transform of the pressure jump across the blade is given by

$$[P(k,0)]^{+}_{-} = -2V/\gamma(k), \tag{A 3}$$

where $$\gamma(k) = [2M^2\Omega k - M^2\Omega^2 + (k_y - \mathrm{i}\epsilon)^2]^{\frac{1}{2}},$$

and the branch cut is chosen to lie between the branch point and infinity in the lower half of the k-plane. The pressure jump (denoted $[p_{2\mathrm{d}}(x,y,0)]^{+}_{-}$) can be recovered by inverting (A 3), and by deforming the contour round the branch cut we find

$$[p_{2\mathrm{d}}(x,y,0)]^{+}_{-} = -V\left(\frac{2}{\pi M^2\Omega x}\right)^{\frac{1}{2}} \exp\left(-\tfrac{1}{4}\mathrm{i}\pi - \tfrac{1}{2}\mathrm{i}\Omega x + \mathrm{i}\frac{xk_y^2}{2M^2\Omega} - \mathrm{i}k_y y\right). \tag{A 4}$$

It follows from (A 3) that the acoustically weighted lift, $\mathscr{L}_{2\mathrm{d}}(y,K)$, is given by

$$\mathscr{L}_{2\mathrm{d}}(y,K) = \frac{2\mathrm{i}V\exp(-\mathrm{i}k_y y)}{(M^2\Omega^2 - k_y^2 + 2M^2\Omega K)^{\frac{1}{2}}}. \tag{A 5}$$

Now considering the radiation we have that the pressure (denoted by $p_{2\mathrm{d}}(x,y,z)$) is given by

$$p_{2\mathrm{d}}(x,y,z) = \mp\frac{V}{2\pi}\int \frac{\exp(-\mathrm{i}kx - \mathrm{i}k_y y - \gamma|z|)}{(2M^2\Omega k - M^2\Omega^2 + k_y^2)^{\frac{1}{2}}}\,\mathrm{d}k, \tag{A 6}$$

where the integration contour lies along the real k-axis, indented above the branch point at $k = (M^2\Omega^2 - k_y^2)/2M^2\Omega$. Deforming the contour onto a path round the branch cut leads to the exact result for the pressure

$$p_{2\mathrm{d}}(x,y,z) = \mp\frac{V}{(2M^2\Omega\pi x)^{\frac{1}{2}}}\exp\left(-\tfrac{1}{4}\mathrm{i}\pi - \tfrac{1}{2}\mathrm{i}\Omega x - \mathrm{i}\frac{M^2\Omega z^2}{2x} + \mathrm{i}\frac{xk_y^2}{2\Omega M^2} - \mathrm{i}k_y y\right), \tag{A 7}$$

which is valid through all space, and in particular in the far field. It can easily be checked that (A 4), (A 5) and (A 7) scale on M in accordance with the transonic similarity law (5).

Appendix B

In this appendix we outline how the results for the acoustically weighted lift per unit span obtained in §5 can be used in predicting either the tip-vortex or the wake interaction noise generated by a counter-rotation propeller. For both noise sources the disturbance shed by the front row, which is then incident on the rear row, can be decomposed into its Fourier components, each corresponding to a harmonic velocity gust of the kind considered in this paper. Working in a frame in which the rear row is fixed, the n_1th harmonic of the incident disturbance has reduced frequency

$$\Omega = 2n_1 BM_{\mathrm{t}} c/(M_{\mathrm{r}} D), \tag{B 1}$$

where B is the blade number (assumed the same for each row), M_{t} is the *rotational* Mach number of the blade tips (again assumed equal in magnitude for the two rows), c is the local chord length of the second-row blades and D is the propeller diameter; full details are given in Parry & Crighton (1989*a*). The reduced frequency is therefore a function of propeller radius. If we consider the n_2th harmonic component of the

radiation produced by the interaction between this n_1th harmonic and the rear row, then the first step in estimating the noise is the calculation of a *chordwise non-compactness factor*, defined by

$$\Psi(y,K) = \int_0^1 [p(x,y,0)]^{\pm} \exp(-\mathrm{i}Kx)\,\mathrm{d}x, \tag{B 2}$$

at each radial station along a given blade in the second row; x and y are the coordinates considered earlier (in the notation of this paper y now corresponds to the coordinate along the propeller radius), $[p(x,y,0)]^{\pm}$ is the unsteady lift distribution due to the interaction with the harmonic gust (which, unlike the lift distribution calculated in this paper, is that of a finite chord blade), and the integration in (B 2) is along the blade chord running from 0 at the leading edge to 1 at the trailing edge. The wavenumber K accounts for the retarded time differences along the blade chord; we have

$$K = \frac{2M_t Bc}{M_r D}\left[\frac{n_1+n_2}{1-M_x\cos\vartheta} - 2n_1\right], \tag{B 3}$$

where M_x is the translational (flight) Mach number of the propeller, M_r is the local helical Mach number of the blade section being considered, and ϑ is the angle between the observer–propeller vector and the flight direction. In modern propeller systems the blade number B is large, allowing the application of asymptotic analysis in the limit $B \to \infty$ (see Parry & Crighton 1989*a*, *b*; Peake & Crighton 1991 for full details), and from (B 3) we therefore see that $\Psi(y,K)$ can be approximated asymptotically in the limit $K \to \infty$ (for certain special-case values of the parameters n_1, n_2, M_x and $\cos\vartheta$ it might be that $K \approx 0$ even for large B, but this will not be considered here). In this limit, $\Psi(y,K)$ will be dominated by contributions from the leading edge (i.e. from the vicinity of the singularity in the lift distribution at $x = 0$), and we can therefore replace the upper limit of the integral in (B 2) by infinity. Moreover, since the effects of the trailing edge will be insignificant in this limit, we can substitute into (B 2) the values of $[p(x,y,0)]^{\pm}$ for the quarter-plane, and therefore have that in the large-blade-number limit

$$\Psi(y,K) \sim \mathscr{L}(y,K);$$

a closed-form algebraic expression for $\mathscr{L}(y,K)$ has already been given in §5.

Once the chordwise non-compactness factor has been determined along the rear-row blade, the noise of a single interaction tone can be evaluated by integrating $\Psi(y,K)$ along the blade span, with inclusion of an appropriate Bessel function factor to account for the radial phasing (see Parry & Crighton 1989*a*). The fact that the theory developed in this paper (and hence our expression for $\mathscr{L}(y,K)$) is only valid for transonic flow speeds, and therefore cannot be valid along the whole blade radius, is of little significance. In typical modern systems operating at cruise, the blade tips certainly move in the transonic regime; in the case of the blade–vortex interaction noise, the portion of the rear-row blades inboard of the tip is not important anyway; whilst for the wake interaction noise, a theory already exists for predicting the blade response away from the tips, and our results would be used to take account of the tip region.

REFERENCES

ABRAMOWITZ, M. & STEGUN, I. A. 1968 *Handbook of Mathematical Functions.* Dover.

AMIET, R. K. 1976 High frequency thin-airfoil theory for subsonic flow. *AIAA J.* **14**, 1076–1082.

AMIET, R. K. 1986 Airfoil gust response and the sound produced by airfoil–vortex interaction. *J. Sound Vib.* **107**, 487–506.

CARGILL, A. M. 1987 Tip effects in the interaction of gusts and vortices with a wing at $M = 1$. *Rolls-Royce Theoret. Sci. Group Rep.* TSG 0294.

CHU, S. & WIDNALL, S. E. 1974 Lifting-surface theory for a semi-infinite wing in oblique gust. *AIAA J.* **12**, 1672–1678.

FFOWCS WILLIAMS, J. E. & GUO, Y. P. 1988 Sound generated from the interruption of a steady flow by a supersonically moving aerofoil. *J. Fluid Mech.* **195**, 113–135.

GOLDSTEIN, M. E. 1976 *Aeroacoustics.* McGraw-Hill.

GRADSHTEYN, I. S. & RYZHIK, I. M. 1980 *Table of Integrals, Series and Products.* Academic.

GUO, Y. P. 1990 Sound generated by a supersonic aerofoil cutting through a steady jet flow. *J. Fluid Mech.* **216**, 193–212.

HANSON, D. B. & PATRICK, M. P. 1989 Near wakes of advanced turbopropellers. *AIAA Paper* 89–1095.

JONES, D. S. 1966 *Generalised Functions.* McGraw-Hill.

JONES, D. S. 1986 *Acoustic and Electromagnetic Waves.* Oxford University Press.

LANDAHL, M. 1989 *Unsteady Transonic Flow.* Cambridge University Press.

MARTINEZ, R. & WIDNALL, S. E. 1980 Unified aerodynamic-acoustic theory for a thin rectangular wing encountering a gust. *AIAA J.* **18**, 636–645.

MARTINEZ, R. & WIDNALL, S. E. 1983 Aerodynamic theory for wing with side edge passing subsonically through a gust. *AIAA J.* **21**, 808–815.

MILES, J. W. 1951 The oscillating rectangular airfoil at supersonic speeds. *Q. Appl. Maths.* **9**, 47–65.

MILES, J. W. 1954 Linearisation of the equations of non-steady flow in a compressible fluid. *J. Math. & Phys.* **33**, 135–143.

NOBLE, B. 1958 *Methods Based on the Wiener–Hopf Technique.* Pergamon.

PARRY, A. B. & CRIGHTON, D. G. 1989*a* Prediction of counter-rotation propeller noise. *AIAA Paper* 89–1141.

PARRY, A. B. & CRIGHTON, D. G. 1989*b* Asymptotic theory of propeller noise – Part I: subsonic single-rotation propeller. *AIAA J.* **27**, 1184–1190.

PEAKE, N. & CRIGHTON, D. G. 1991 An asymptotic theory of near-field propeller acoustics. *J. Fluid Mech.* **232**, 285–301.

REYNOLDS, B. D. 1979 Characteristics of the wake of a lightly loaded compressor or fan blade. *AIAA Paper* 79–0550.

SIMONICH, J. C., MCCORMICK, D. C. & LAVRICH, P. L. 1989 Interaction noise mechanisms for advanced propellers experimental results. *AIAA Paper* 89–1093.

STEWARTSON, K. 1950 On the linearized potential theory of unsteady supersonic motion. *Q. J. Mech. Appl. Maths.* **3**, 182–199.

SUNDAR, R. M. & SULLIVAN, J. P. 1986 An experimental investigation of propeller wakes using a laser Doppler velocimeter. *AIAA Paper* 86–0080.

VACZY, C. M. & MCCORMICK, D. C. 1987 A study of the leading edge vortex and tip vortex on prop-fan blades. *J. Turbomachinery* **109**, 325–331.